GEOLOGICAL SURVEY OF CANADA
OPEN FILE 7853

Targeted Geoscience Initiative 4: Contributions to the Understanding of Volcanogenic Massive Sulphide Deposit Genesis and Exploration Methods Development

Oxygen isotope zonation about the Izok Ag-VMS deposit, Slave Province, Nunavut: hanging-wall vector to mineralization

Bruce E. Taylor[1], Jan M. Peter[1], Kati Laakso[2,3], and Benoit Rivard[2]

[1]Geological Survey of Canada, Ottawa, Ontario
[2]University of Alberta, Edmonton, Alberta
[3]Spectral Imaging Ltd., Oulu, Finland

2015

This publication is available for free download through GEOSCAN (http://geoscan.nrcan.gc.ca/)

Recommended citation
Taylor, B.E., Peter, J.M., Laakso, K., and Rivard, B., 2015. Oxygen isotope zonation about the Izok Ag-VMS deposit, Slave Province, Nunavut: hanging-wall vector to mineralization, *In:* Targeted Geoscience Initiative 4: Contributions to the Understanding of Volcanogenic Massive Sulphide Deposit Genesis and Exploration Methods Development, (ed.) J.M. Peter and P. Mercier-Langevin; Geological Survey of Canada, Open File 7853, p. 27–44.

Publications in this series have not been edited; they are released as submitted by the author.

Contribution to the Geological Survey of Canada's Targeted Geoscience Initiative 4 (TGI-4) Program (2010–2015)

TABLE OF CONTENTS

Oxygen isotope zonation about the Izok Ag-VMS deposit, Slave Province, Nunavut: hanging-wall vector to mineralization

Bruce E. Taylor[1]*, J.M. Peter[1], Kati Laakso[2,3], and Benoit Rivard[2]

[1]Central Canada Division, Geological Survey of Canada, 601 Booth Street, Ottawa, Ontario K1A 0E8
[2]Centre for Earth Observation Sciences at the University of Alberta, Department of Earth and Atmospheric Sciences,
  University of Alberta, 1-26 Earth Sciences Building, University of Alberta, Edmonton, Alberta T6G 2E3
[3]SPECIM, Spectral Imaging Ltd., Teknologiantie 18 A FI-90590 Oulu, Finland
*Corresponding author's e-mail: btaylor@nrcan-rncan.gc.ca

ABSTRACT

Oxygen isotope compositions were determined for 99 whole-rock samples of felsic host rocks collected in the vicinity of the Izok volcanogenic massive sulphide deposit. The results reveal a distinct pattern of oxygen isotope zonation spatially centred over the massive sulphide lenses produced by water/rock reaction in a hydrothermal system. The zonation indicates that this paleo-hydrothermal system is relatively 'up right', centered over the massive sulphide lenses. Analyzed samples are primarily from the hanging wall, and have $\delta^{18}O_{V-SMOW}$ values as high as 14.7‰. In contrast to isotopic studies describing ^{18}O-depleted footwall and upflow zones, the ^{18}O-enriched zoning pattern in the Izok Lake area illustrates a clear hanging-wall "vector" to the buried sulphide lenses. This isotopic 'fingerprint' of an Archean hydrothermal system has been retained in the rocks, despite subsequent amphibolite facies metamorphism. The isotopic zonation broadly corresponds to an isopleth indicating loss of Na_2O from the rocks, and, to some extent, with a mapped distribution of the Ishikawa alteration index and short-wave infrared spectral mapping of white-mica and biotite+chlorite-related absorption features. However, the pattern of oxygen isotope zonation provides a more focused 'target'.

INTRODUCTION

Submarine, magmatic-centred hydrothermal systems profoundly alter the isotopic, mineralogical, and chemical compositions of host igneous and sedimentary rocks. Subsequent metamorphism and deformation can modify the chemical and physical properties of the altered rocks further. Oxygen isotope techniques can be used to map the morphology of volcanogenic massive sulphide (VMS)-associated submarine hydrothermal systems and provide a robust, quantitative parameter with which to determine the paleo-architecture of the hydrothermal system, including flow paths and thermal gradients. Isotopic mapping of these features offers a 'fingerprint' that can be used as an exploration 'vector'. As established in other studies of VMS systems, oxygen isotope alteration and zoning survives metamorphic recrystallization and deformation, although the morphologies of the oxygen isotope zones may reflect associated strain (e.g. Sturgeon Lake: Holk et al., 2008; Snow Lake: Taylor and Timbal, 1998a; Bailes et al., in press). Herein we summarize the results of an oxygen isotope study of the Izok Lake paleo-hydrothermal system, host to a large, undeveloped Zn-Cu VMS deposit. The study reveals a zone of signifi-cant oxygen isotope enrichment in hanging-wall rocks that can serve as vector to the buried Zn-Cu-Pb-Ag volcanogenic massive sulphide ore bodies. Furthermore, the data provide a framework for comparison to other chemical, mineralogical and spectral rock properties of the hydrothermal alteration zones at Izok Lake that collectively can be used to construct more comprehensive exploration methods.

LOCATION AND GEOLOGICAL SETTING

The Izok deposit is located in southwestern Nunavut, and is hosted primarily by metamorphosed rhyolitic rocks Archean age and, to a lesser extent, by intermediate to mafic metavolcanic and metasedimentary rocks of the Point Lake greenstone belt within the Slave Craton (also referred to herein as the Slave Province; Fig. 1). Mortensen et al. (1988) determined an Archean U/Pb zircon age of 2623 Ma for rhyolite in the Izok Lake area. Bailey and Stubley (2013a,b) divided the assemblage of rhyolitic rocks into 7 units on the basis of lithogeochemistry, noting that the rocks largely represent reworked and re-sedimented volcanic and volcaniclastic detritus. The stratigraphically lowest rhyolitic unit (R1), hosts the Izok deposit.
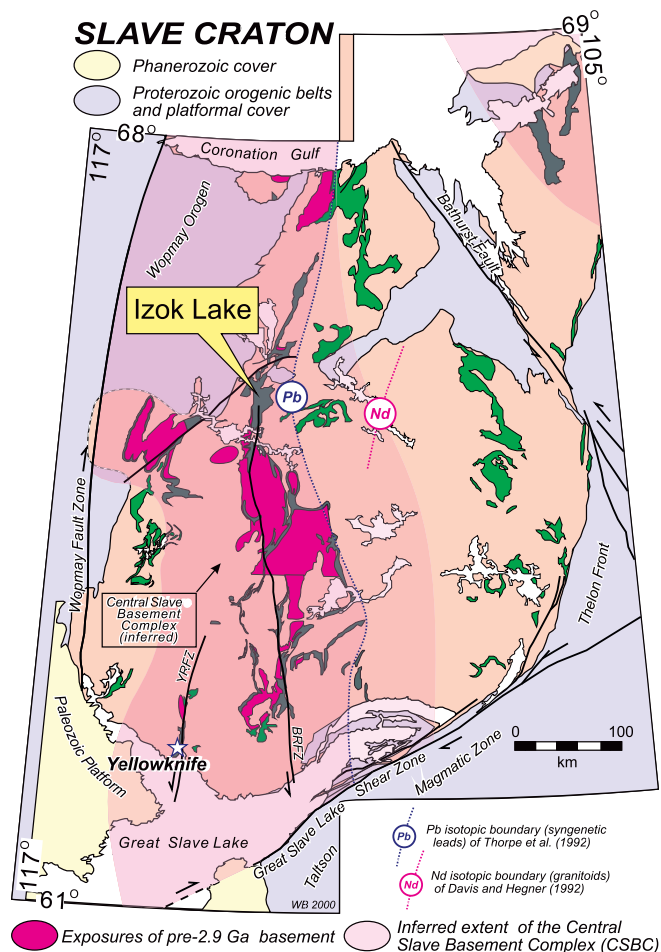
Figure 1. Geological map of the Slave craton (province; modified after Bleeker and Hall, 2007) showing the location of the Izok Zn-Cu-Pb-Ag VMS deposit (65°37.5'N; 112°48.0'W), in the Kitikmeot region of Nunavut. The deposit represents a resource of 15 Mt grading 13% Zn, 2.3% Cu, 1.4% Pb, and 73 g/t Ag (MMG, Inc., Annual Report 2013).

Massive sulphides were discovered at Izok Lake in 1974 by Texasgulf, Inc., intercepting massive sulphide in the first drill hole (Morrison, 2004). The name 'Izok' was derived from "Is OK" reference used by early explorationists (Morrsion, 2004). The deposit consists of five sulphide lenses comprising a current resource of 15 Mt grading 13% Zn, 2.3% Cu, 1.4% Pb, and 73 g/t Ag (MMG Inc., Annual Report 2013).

The simplified geological map of the Izok Lake Area, shown in Figure 2, illustrates the dominance of rhyolitic flows and volcaniclastic rocks. Four generations of folds have been interpreted of the area as the result of a complex deformational history (Stubley and Bailey, 2013); only the last two generations, F_3 and F_4, are represented in Figure 2. The F_3 antiform aligned with the massive sulphide lenses is subparallel to many, smaller F_2 folds. The axial planes of these folds are generally upright, to slightly northwest-tilted. The axis of a broad, arching fold at a high angle to the general trends of the F_2-F_3 folds represents the last episode of

folding (Stubley and Bailey, 2013); the domical apex formed by the intersection the F_3 and F_4 folds is located in the vicinity of the massive sulphide lenses. Consequently, the F_3 fold axis is shown as doubly-plunging, although fold axes in the area are generally sub-horizontal to shallow dipping (Bailey and Stubley, person. comm.). A region of sillimanite- and garnet-bearing rocks (amphibolite-grade metamorphic equivalents of hydrothermally altered rocks) southwest of the sulphide lenses appears to be situated along the axis of the F_3 antiform (Fig. 2).

Only rhyolitic rocks throughout the area were analyzed for their oxygen isotope compositions in order to provide a sensitive means of mapping the VMS-related paleo-hydrothermal system. A typical outcrop exposure is shown in Figure 3a, which illustrates a well-developed, penetrative schistosity in hydrothermally altered rocks. Outcrops are typically densely covered with lichen. Figure 3b shows volcaniclastic textures in an outcrop that was power-washed to remove the lichen. Photographs in Figure 3c and 3d illustrate the porphyblastic textures of garnet- and sillimanite-bearing mineral assemblages characteristic of metamorphosed hydrothermally altered rocks.

SAMPLE SELECTION AND METHODOLOGY

A total of 99 samples, consisting of 85 representative hand samples or chip collections from surface outcrops and 14 samples collected from selected drill core, were analyzed for their oxygen isotope compositions in this study. Surface samples were collected throughout much of the Izok Lake area, within 8 km of the VMS lenses (Fig. 2); however, samples from drill core were only collected in the immediate vicinity of the VMS lenses.

Analysis of aliquots of 5–15 mg of dried rock powder were carried out by standard fluorination methods employing ClF_3 (Borthwick and Harmon, 1982; Taylor, 2004). Oxygen isotope compositions are reported in the usual δ-notation, relative to V-SMOW (Vienna Standard Mean Ocean Water), and considered accurate to better than 0.2 per mil (‰, 1σ). Analyses were performed at the University of Western Ontario, London. Consistency among the data was monitored by analysis of common internal working standards, international reference materials, and blind duplicates.

The oxygen isotope data acquired in the present study were compared to spectral measurements from Laakso et al. (2015) made on the same samples or outcrops. Spectra were acquired in the field with a hand-held ASD FieldSpec® Pro 3 spectrometer (hereafter referred to as "ASD"). The ASD records spectra in the 350–2500 nanometres (nm) wavelength range with a spectral resolution of 10 nm in the short-wave infrared
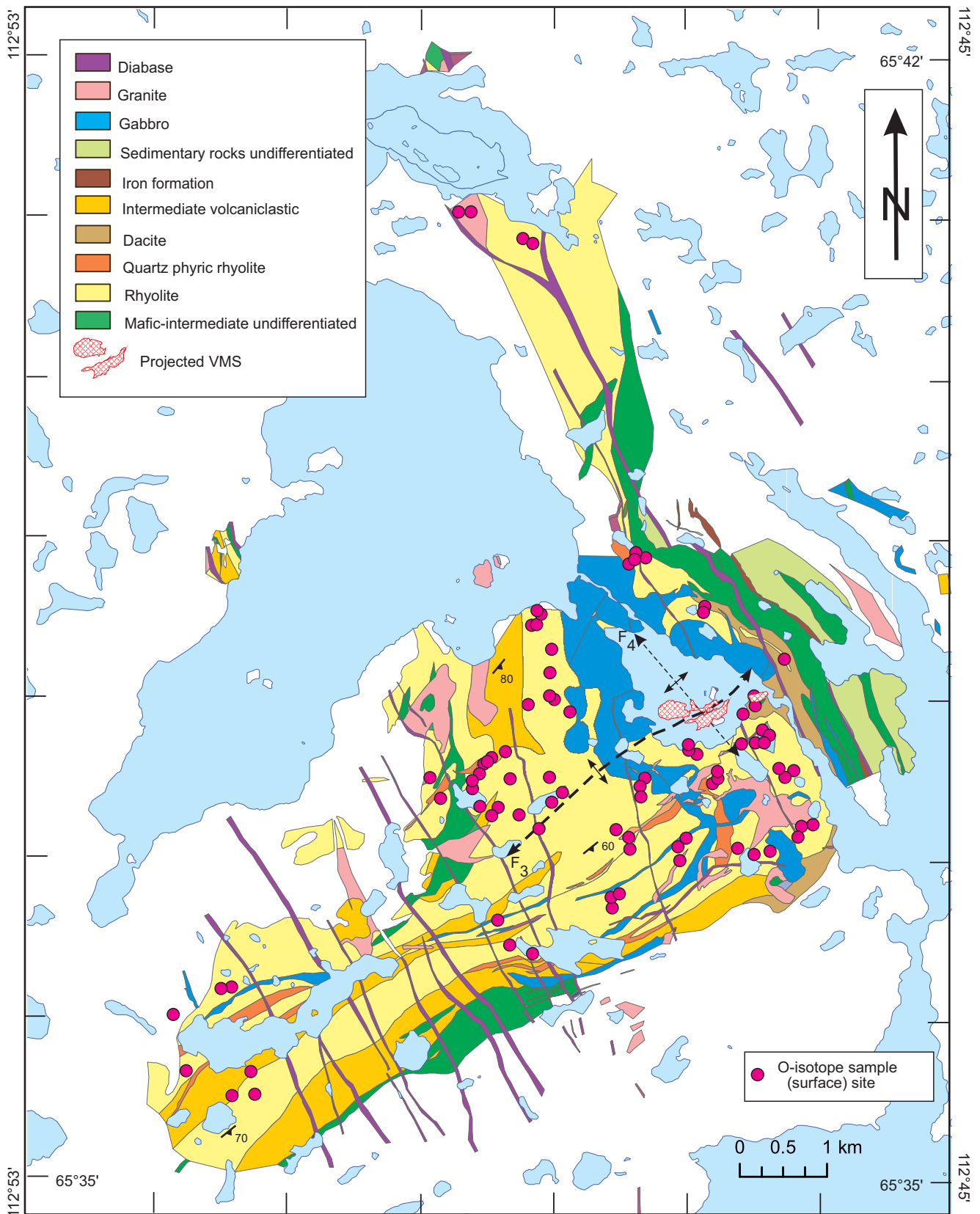
Figure 2. Simplified regional geological map of the Izok Lake area, Nunuavut (based on Stubley and Bailey, 2013, after Inmet, unpub.; Minerals and Metals Group, Ltd.), showing the locations of 99 surface-collected whole-rock samples from the hanging wall to the deposit, which were analysed in this study for their oxygen isotope compositions. An additional 14 samples were analyzed from drill core (see Fig. 9). The buried VMS bodies comprising the Izok deposits are represented by projection (Minerals and Metals Group, Ltd., unpub.). See text for discussion of F_3 and F_4 folds.
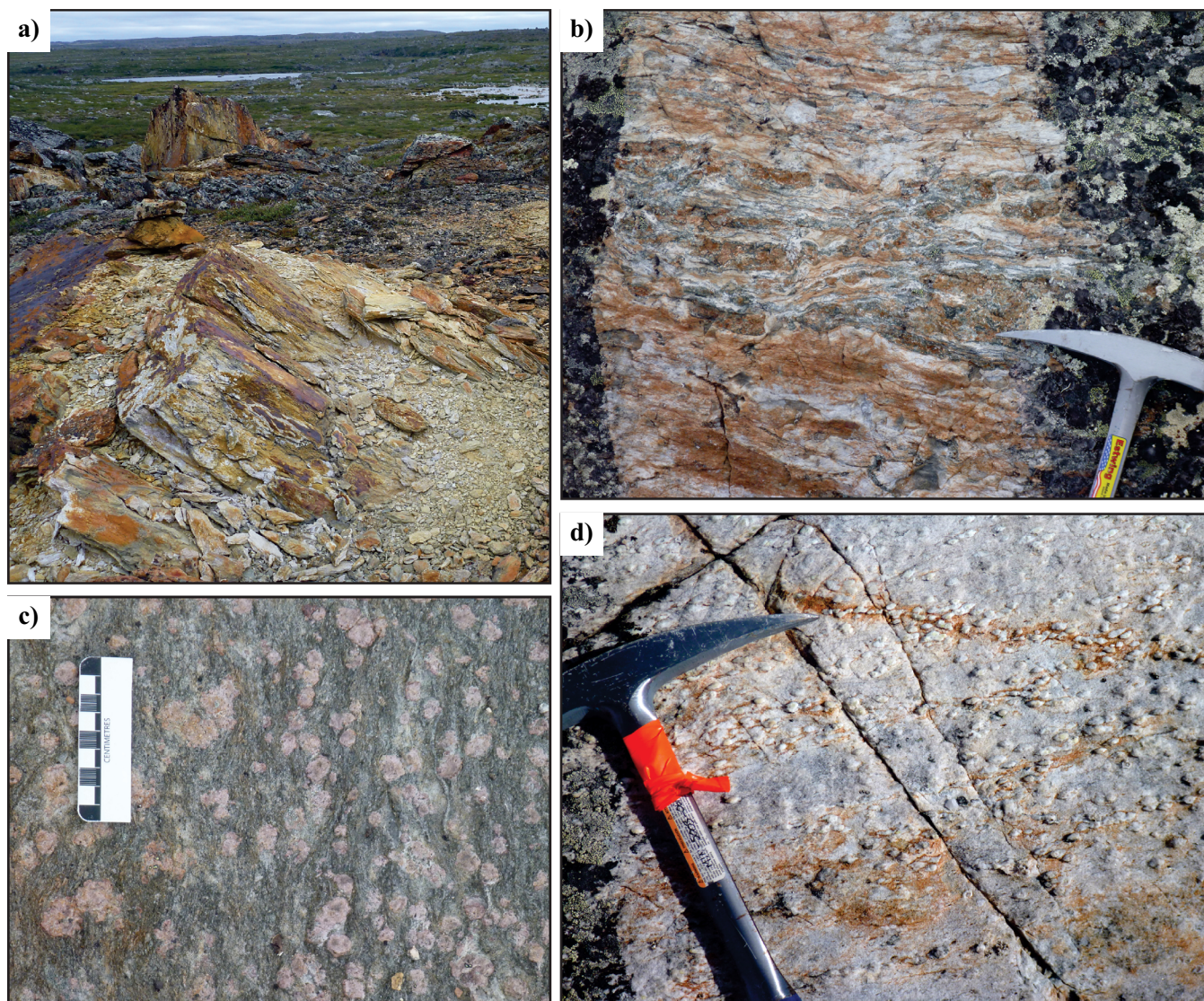
Figure 3. Outcrop photographs of rhyolitic rocks in the Izok Lake area. **a)** Rust-stained, sericite-altered, rhyolitic volcaniclastic rocks in outcrop with schistose parting. **b)** Power-washed exposure of foliated rhyolitic volcaniclastic rock with siliceous clasts in chlorite-bearing matrix. **c)** Garnet porphyroblasts decorate this power-washed exposure of foliated, chlorite-bearing rhyolite. **d)** Clots of sillimanite in muscovite-rich meta-rhyolite (some muscovite of retrograde origin envelopes sillimanite) attest to a high metamorphic grade.

wavelength region. The spectra were acquired with a fore optic contact probe. Radiance values were converted to reflectance values by means of a Spectralon™ (Labsphere, New Hampshire, U.S.A.) 99% panel. The geographic locations of the field sites were recorded with a handheld GPS.

RESULTS

The geographic distribution of isotopic compositions of the 85 analysed surface samples, grouped in 2‰ fashion, is shown in Figure 4. The $\delta^{18}O$ values of the surface samples vary from 5.8 to 14.7‰; only three samples have $\delta^{18}O$ values of <6‰ (Figs. 4, 5). As indicated in Figure 4, rocks having the lowest $\delta^{18}O$ values (<6‰, but only by a few tenths per mil; 5.8‰) are among the most distal from the VMS lenses, and represent fresh rhyolite. Typically, mantle-derived fresh, unaltered rhyolite has oxygen isotope compositions of ~6–7.5‰ (e.g. Taylor, 1968). Rhyolite that has values of $\delta^{18}O > 9‰$ (light- and dark-blue coded, and many of the green-coded samples in Fig. 4) are isotopically enriched relative to fresh, unaltered rhyolite as a result of hydrothermal alteration. The histogram shown in Figure 5 for surface samples and drill-core samples illustrates that the majority of samples analysed have $\delta^{18}O$ values > 9‰; indeed, the mean value of $\delta^{18}O$ is 10.16‰. Fourteen drill-core samples within the vicinity of Izok VMS lenses have a somewhat restricted range of $\delta^{18}O$ from 8.9 to 12.4‰, centred about the mean value for all samples. The significance of this distribution is discussed later.
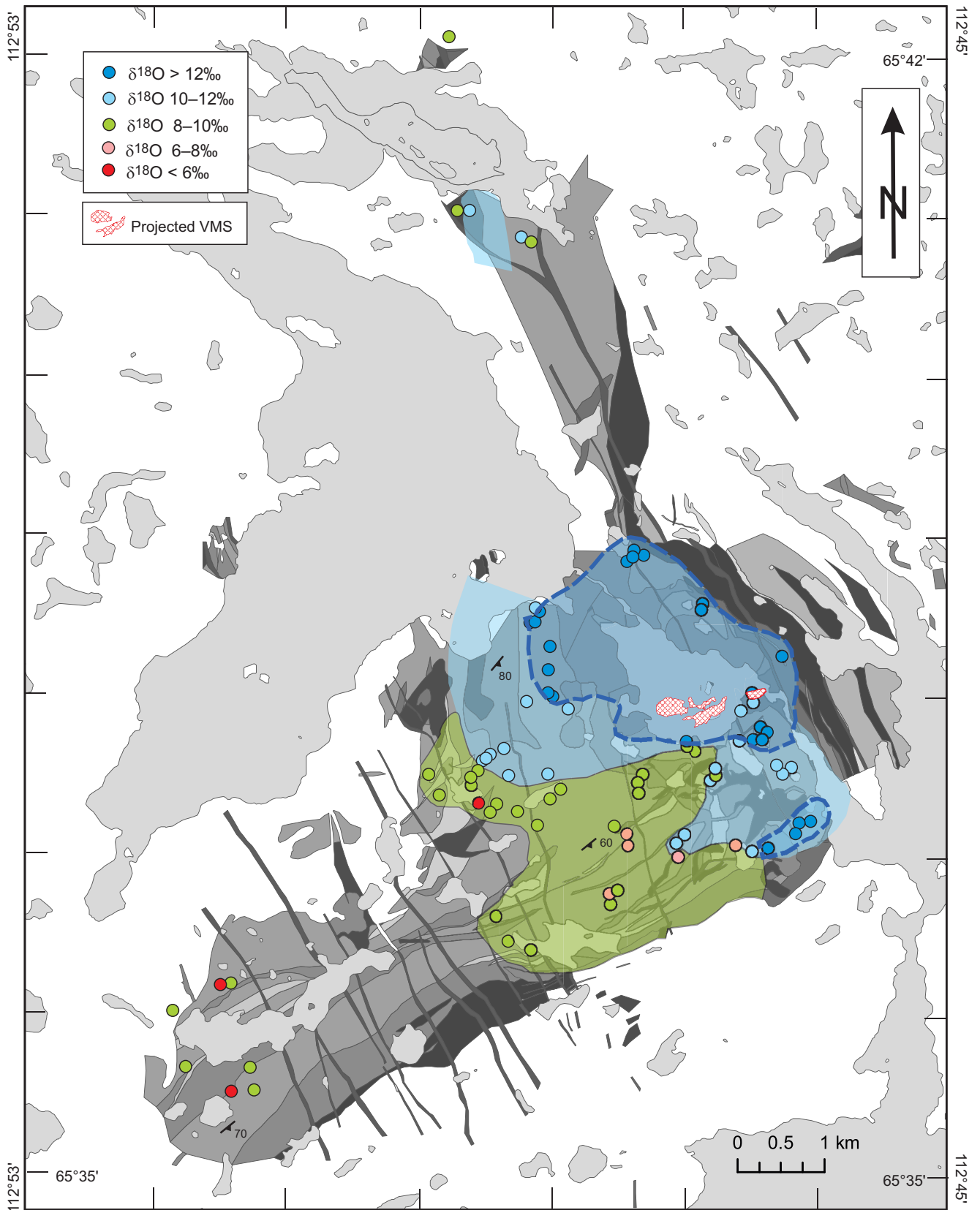
Figure 4. Geological map of Izok Lake area, showing site locations of analyzed rhyolite samples, colour-coded using 2‰ brackets to represent isotopic variation. See Figure 2 for a coloured version of the geological map. Note the increase in whole-rock δ18O values as the VMS lenses (surface projections: MMG, Inc.) are approached.
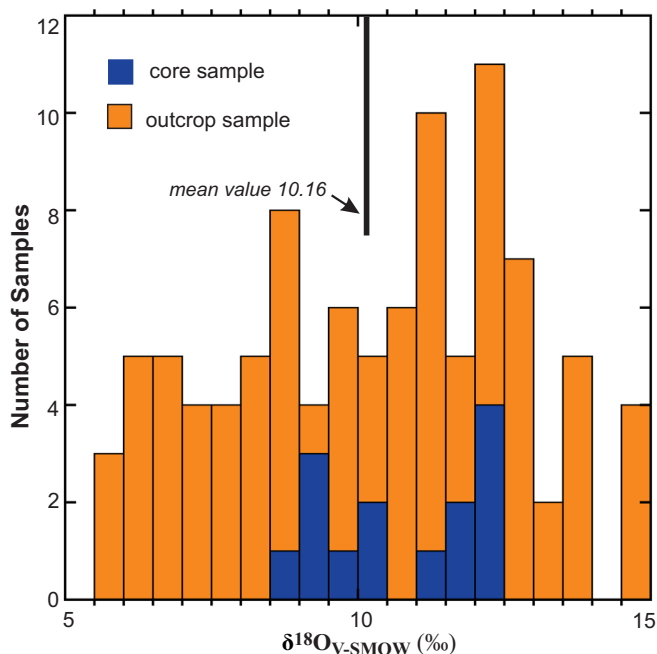
Figure 5. Histogram of whole-rock oxygen isotope compositions for rhyolite samples collected from surface outcrops (n=85) in the Izok Lake area and from drill core (n=14;) in the vicinity of the Izok massive sulphide lenses. The distribution represents a range of $\delta^{18}O$ = 5.8 to 14.7‰. Fresh rhyolite (and, permissibly, those slightly altered by seawater at moderate temperatures) typically has $\delta^{18}O$ values of ~6-7‰, whereas, rocks with heavier isotopic compositions, especially ≥ 9‰, have been hydrothermally altered at low to moderate temperatures (see text).

DISCUSSION

Water-Rock Interaction

The effects of oxygen isotope exchange between hydrothermal fluids and volcanic and sedimentary rocks in seawater-dominated hydrothermal systems have been documented systematically over the last several decades. A brief review here of the systematics and several examples provides background essential to a discussion of the Izok Lake VMS hydrothermal system.

The progressive oxygen isotope exchange between seawater ($\delta^{18}O$ = 0‰) and fresh volcanic rocks (e.g. rhyolite and andesite; $\delta^{18}O$ ≈ 6 and 7.5‰, respectively; Taylor, 1968) is depicted in Figure 6 as a function of the integrated water/rock ratio (W/R). In this diagram the isotopic compositions of rhyolite and andesite are shown on the left ordinate, and seawater on the right ordinate. The change in composition of each (rocks and water) then varies as a function of temperature and cumulative isotopic exchange accompanying chemical and mineralogical changes to the rock during hydrothermal alteration. The oxygen isotope composition of unaltered rhyolite and andesite may vary slightly (generally 1–2‰) from that shown here as a function of source materials and tectonic setting (e.g. Sheppard and Taylor, 1986; Taylor, 1986). It is the min-
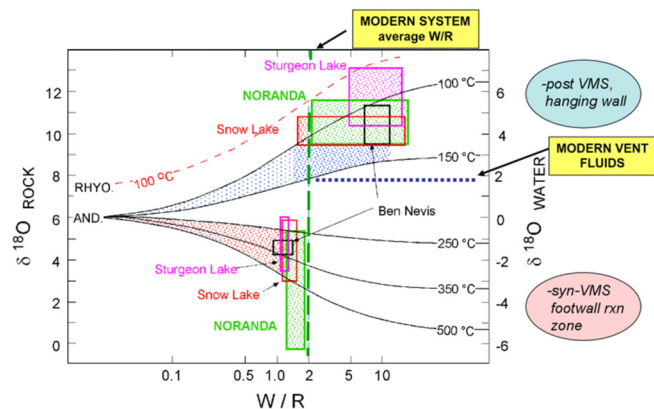

Figure 6. Plot of whole-rock oxygen isotope alteration (variation of $\delta^{18}O_{ROCK}$; RHYO.= rhyolite, AND.= andesite) and seawater hydrothermal fluid ($\delta^{18}O_{WATER}$) as a function of integrated water/rock ratio (W/R) during hydrothermal alteration. Rock alteration begins at the left side of the diagram, with the $\delta^{18}O_{ROCK}$ and $\delta^{18}O_{WATER}$ changing along the pathways shown as hydrothermal alteration occurs. At high temperatures, $\delta^{18}O_{ROCK}$ decreases, recording a measurable alteration signature in the footwall. Low-temperature alteration may be recorded in the hanging wall if the rocks are deposited before cessation of hydrothermal activity. Fields for whole-rock isotopic compositions (both high and low temperature) from several studied examples (see Holk et al., 2008; Taylor et al., 2009) and selected reference points from modern systems are shown.

eralogical alteration of the rocks (particularly, glassy components) that promotes significant oxygen isotope exchange. The oxygen isotope composition of the whole-rock, determined by the mineralogical mode and the individual mineral-water oxygen isotope fractionation factors, is strongly influenced by the abundance of dominant alteration minerals such as chlorite or muscovite. Note that at low to moderate values of W/R, the whole-rock oxygen isotope composition remains within the general range of fresh, isotopically 'unaltered' rocks because feldspar-water fractionation factors (which can play a significant role in this scenario) are relatively small in the 200–250°C range. Several reference points are shown in Figure 6, including an average oxygen isotope composition of ≈ 2‰ for modern vent fluids (e.g. Shanks, 2001). Vent fluids have positive values of $\delta^{18}O$ because of water/rock interaction along the flow paths in the hydrothermal systems. Figure 6 can be used to estimate W/R ratios from comparison of the oxygen isotope compositions of fresh and altered rocks.

The results of comprehensive oxygen isotope studies of a number of felsic magmatic-centred mineralized and non-mineralized sea floor hydrothermal systems, plotted as fields for both high- and low-temperature zones (i.e. <6 and >9‰), are compared in Figure 6. In general terms, the size and distribution of the plotted zones illustrates the size and complexity of the individual hydrothermal systems and, with the exception of
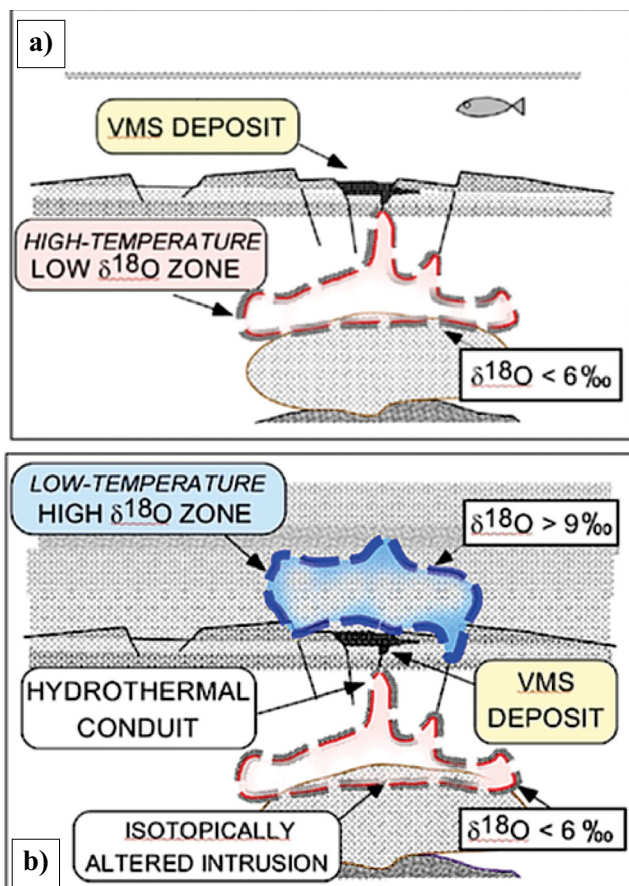
Figure 7. a) Schematic cross-section of the formation of a high-temperature reaction zone associated with a subvolcanic intrusion, characterized by a low $\delta^{18}O$ zone in a marine hydrothermal system (Taylor et al., 2009). Most unaltered volcanic rocks have $\delta^{18}O$ values of 6-9‰; high-temperature alteration is indicated by $\delta^{18}O < 6‰$. Distribution of the high-temperature alteration zone records hydrothermal fluid flow. The zone may collapse on high-temperature heat source (e.g. synvolcanic pluton, locally crystallized and fractured), which may be up to 1–2 km beneath the seafloor (e.g. Galley et al., 2007). Synvolcanic faults that acted as hydrothermal conduits ("feeder zones") may be identified by lowered values of $\delta^{18}O$. **b)** Schematic cross-section of the formation of a low-temperature, high-$\delta^{18}O$ zone in a marine hydrothermal system. Lower temperature alteration is typically indicated by $\delta^{18}O_{WR} > 9‰$. Note that volcanism and/or sedimentation must continue during the waning of the hydrothermal system to record lower-temperature alteration. A high-$\delta^{18}O$ "cap" may develop in the hanging wall, above the upflow zone in the footwall, providing a hanging-wall "vector" to guide exploration. Examples of high-$\delta^{18}O$ hanging-wall indicators of buried VMS may be found at Sturgeon Lake, Ontario (Holk et al., 2008), Flin Flon, Manitoba. (Ames et al., in press), and Snow Lake, Manitoba. (Taylor and Timbal, 1998b; Bailes et al., in press).

Noranda, represent single episode systems. High-temperature alteration is designated as a syn-VMS reaction zone in Figure 6 because it develops at depth as the VMS deposit(s) form at or near the sea floor in rocks that are, except along narrow fluid pathways, not significantly isotopically altered (Taylor and Holk, 1998).

Low-temperature alteration zones are designated as 'post-VMS, hanging wall' and correspond to the hanging-wall zone depicted in Figure 7. In the case of Noranda, the extended, ^{18}O-depleted field represents the combined effects of at least four, superposed episodes of magmatism and hydrothermal activity (Taylor et al., 2009). Consequently, the temperature implied by Figure 6 for water/rock interaction well above 500°C is apparent only.

The Ben Nevis complex in the Noranda camp, shown in Figure 6, has small zones of associated high- and low-temperature alteration. It is an upright pluton, ca. 10 my younger than the Flavrian intrusive complex (Piercey et al., 2008). The orientation of the Ben Nevis paleo-hydrothermal system precluded study of the hanging wall and of any possible effects of volcanogenic mineralization (Taylor and Timbal, 1998a). Still, a small hydrothermal system driven by the heat of the cooling Ben Nevis pluton, produced similar, if restricted, isotopic alteration zones to the larger complexes represented.

Long-lived submarine hydrothermal systems centred on subvolcanic VMS-producing intrusive centres that fuelled long-lived hydrothermal systems can produce a high-$\delta^{18}O$ alteration zone in rocks deposited after most or all of the near surface VMS mineralization has been deposited (see Fig. 7b). This post-VMS hanging-wall feature, is characterized by a range of $\delta^{18}O$ values that, as shown, can be on the order of 9.0 to 13‰. Isotopic alteration at Sturgeon Lake (Holk et al., 2008) provides a particularly useful example of such a post-VMS, high-$\delta^{18}O$ zone in the hanging wall, with $\delta^{18}O$ values of up to 13‰. Continual, shallowing growth and eventual emergence of the volcanic edifice at Sturgeon Lake played an important role in the lower temperature ^{18}O enrichment of the hanging-wall volcanic rocks (Holk et al., 2008).

Oxygen Isotope Zonation in Marine Hydrothermal Systems

Much of the discussion in previously published oxygen isotope studies of VMS hydrothermal systems focussed on the high-temperature, ^{18}O-depleted reaction zones and hydrothermal pathways in the footwalls to deposits (e.g. Larson, 1984; Taylor and South, 1985; Cathles, 1993; Taylor et al., 2009, 2014). Although this is an important isotopic aspect of submarine hydrothermal alteration, it is the lower-temperature alteration systematics and resulting isotopic zoning patterns that are of particular interest in the Izok Lake area. Examples of previously documented high-^{18}O hanging-wall enrichment associated with VMS deposits include: Kuroko deposits, Hokuroku District, Japan (Green et al., 1983), Sturgeon Lake, Ontario (Holk et al, 2008), and LaRonde Penna, Noranda, Quebec (Beaudoin et al.,

2014). The mapping of the distribution of both the high-temperature, ^{18}O-depleted, and low-temperature, ^{18}O-enriched alteration zones can be used in exploration vectoring.

The schematic evolution of oxygen isotope zonation in a simple (i.e. one intrusion/intrusive episode) felsic magmatic-centred submarine hydrothermal system is shown in cross-section in Figure 7. This figure illustrates the spatial relationship of zones of oxygen isotope enrichment to the zone of massive sulphide formation observed in the Izok Lake area. The high-temperature zone of oxygen isotope depletion shown schematically in Figure 7a, as mapped in other paleo-hydrothermal systems, represents the cumulative high-temperature alteration during the life of the hydrothermal system. As such, as the system waxes and wanes, the boundaries can move, up and down, respectively; it may also 'collapse', moving downward, upon the intrusion that provides the thermal drive for hydrothermal circulation as the intrusion crystallizes and fractures at temperatures of ~350°C. In multi-stage, sub-volcanic intrusive complexes, magmatic pulses may invade previously hydrothermally altered portions of the hydrothermal system, stoping and disrupting altered rock.

Hydrothermal circulation will proceed as long as sufficient heat remains to provide the buoyancy to the fluids. In an area of active volcanism, continued volcanism and sedimentation may bury the VMS deposit shortly after (or during) its formation. Lower temperature hydrothermal alteration and, in particular, oxygen isotope alteration may accompany the protracted cooling of the heat source, leaving an imprint on the hanging-wall rocks of higher $\delta^{18}O$ values in areas above fluid upflow zones. As shown in Figure 7b, lower temperature alteration may also affect some rocks in the foot wall. The high-$\delta^{18}O$ zone, or 'cap' above the upflow zone, can provide a vector in the hanging-wall rocks to buried VMS.

The oxygen isotope zonation described above can be employed as an effective tool with which to map the architecture and orientation of a paleo-submarine hydrothermal system. The pattern of mapped oxygen isotope zones indicates the polarity of the system with respect to thermal gradients and fluid flow. The alteration patterns and the location of the VMS depositional zone shown schematically above are sufficiently reliable that the general architecture of paleo-hydrothermal systems may be understood even in the absence of a complete system in the area of interest, providing 'vectors' for exploration.

Oxygen Isotope Zonation at Izok Lake

Sampling and analysis of only rocks of rhyolitic composition in the Izok Lake area permitted use of a finer grouping (2‰) of oxygen isotope composition than the <6 and >9‰ divisions typically used for map contouring purposes (Fig. 8). This approach allowed comparison of the isotopic changes throughout the area of an (originally) isotopically similar rock. Isotopic differences due primarily to different rock compositions (e.g. basalt, andesite, etc.) were thereby eliminated. Consequently, an improved definition of the zone boundaries of oxygen isotope alteration resulted. Figure 9 displays the pattern of oxygen isotope alteration zones in the immediate vicinity of the Izok deposit based on analyses of drill core samples that encompass the projected extent of the buried sulphide lenses. The positions of the zone boundaries in both Figures 8 and 9 are necessarily strongly influenced by the distribution of available analyses; the locations of zone boundaries northeast of Izok Lake are uncertain. The boundaries are also influenced by the inferred folding along northeast-southwest axes, yet the pattern of zoning indicates a moderately upright, only slightly tilted to the northwest, top-down (i.e. plan) view of the paleo-hydrothermal system. We interpret the high-$\delta^{18}O$ zone that encompasses the vertical projections of VMS lenses beneath Izok Lake in Figure 8 to be the low-temperature alteration 'cap' above the upflow zone responsible for the sulphide mineralization (see Fig. 7b). Comparison of the detailed oxygen isotope zonation map (Fig. 9) with that shown in Figure 8 (note the inset outline of Fig. 9) provides the basis for this interpretation.

South of the locations of the projected VMS lenses in Figure 8, there are five samples with oxygen isotope compositions in the 6–8‰ interval, indicating a relatively small zone of isotopically 'normal' rocks. A small zone encompassing these five samples was not drawn for simplicity, although it, like other zones, would have a shape reflecting the northeast-southwest folding.

The three samples with $\delta^{18}O$ values < 6‰ (actually 5.8‰; see Fig. 5) are among the furthest from the VMS lenses. Rather than indicating high-temperature alteration, these samples have an isotopic composition close to that consistent with unaltered rhyolite, or those altered at moderate temperatures (i.e. ~200–250°C; see Fig. 6). Similarly, those sites colour-coded green in Figure 8 represent samples in this "unaltered" group. Collectively, the broad dispersal of 6–8‰ samples contrasts with the more restricted, high-$\delta^{18}O$ zone encircling Izok Lake.

Applying the same $\delta^{18}O$ interval of 2‰ defined as above, isotopic zonation in the immediate vicinity of the buried VMS lenses at the southwestern end of Izok Lake is shown in Figure 9. Whereas, the regional oxygen isotope zonation map in Figure 8 emphasizes the high-$\delta^{18}O$ zone encompassing Izok Lake, the close spacing of drill core samples near and adjacent to VMS lenses permits the definition of a 'central' zone of
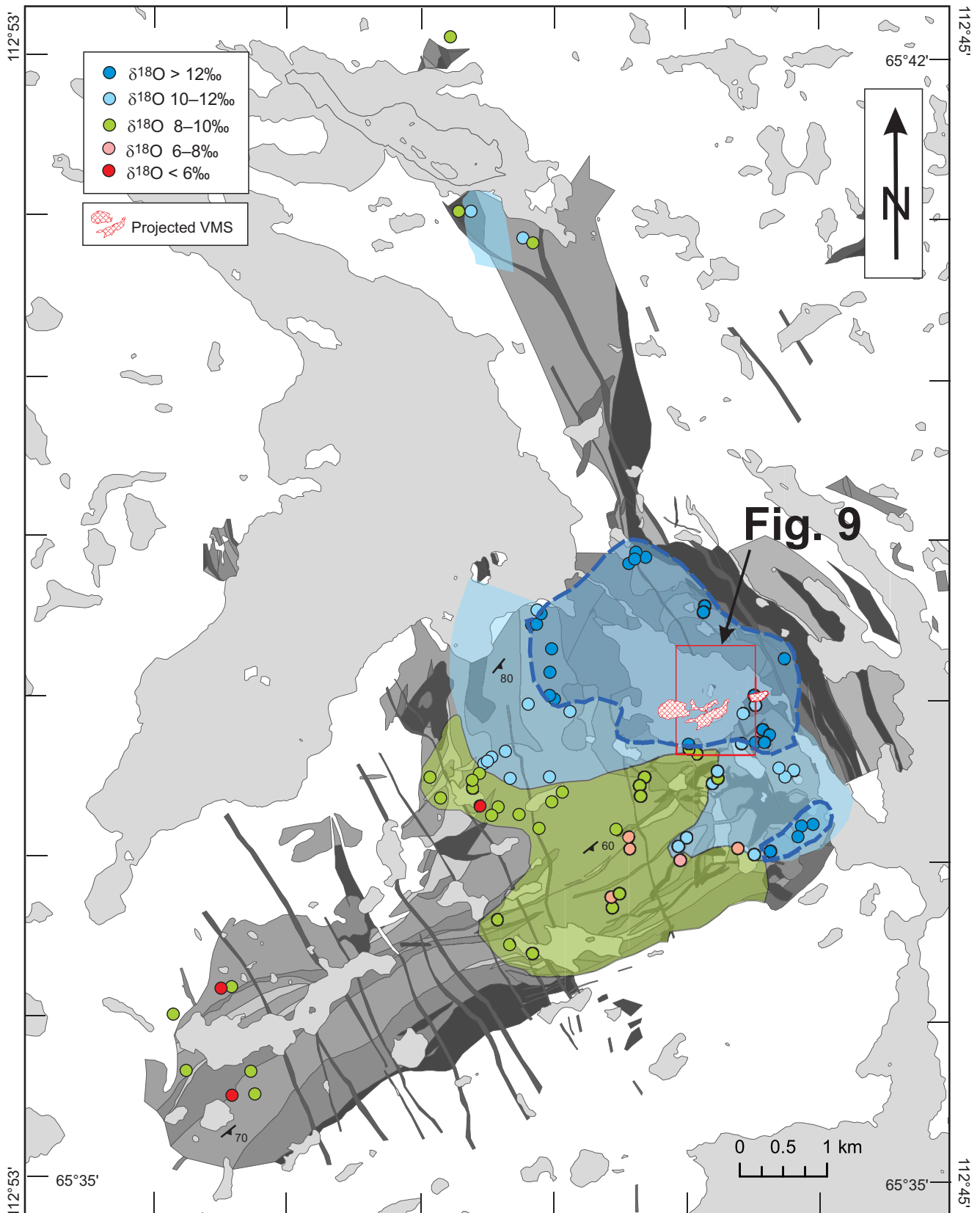
Figure 8. Map of oxygen isotope zonation in the hanging-wall rocks of the Izok Lake area, which encompasses the projections (Bailey and Stubley, 2013a,b) of buried VMS mineralization. The pattern of zoning shown in this figure characterizes a relatively upright hydrothermal system and is viewed from the "top" down (i.e. plan view). The high δ18O (low-temperature) zone provides a hanging-wall target for exploration. A small area of isotopically "normal" rocks is indicated south of the projected VMS bodies; the corresponding zone boundaries are not shown for simplicity. Note the location of Figure 9.

Figure 9. Oxygen isotope zonation in the vicinity of VMS bodies based on analyses of samples from drill core. The location of this area is indicated by an inset frame in Figure 8. A relative decrease in $\delta^{18}O_{WR}$ closely associated with the VMS, in an otherwise isotopically enriched zone, is likely located above a more deeply buried upflow zone. The drillholes shown were all less than 600 m in depth, limiting access to the footwall. In most cases, samples were collected within several hundred metres of mass sulphide.

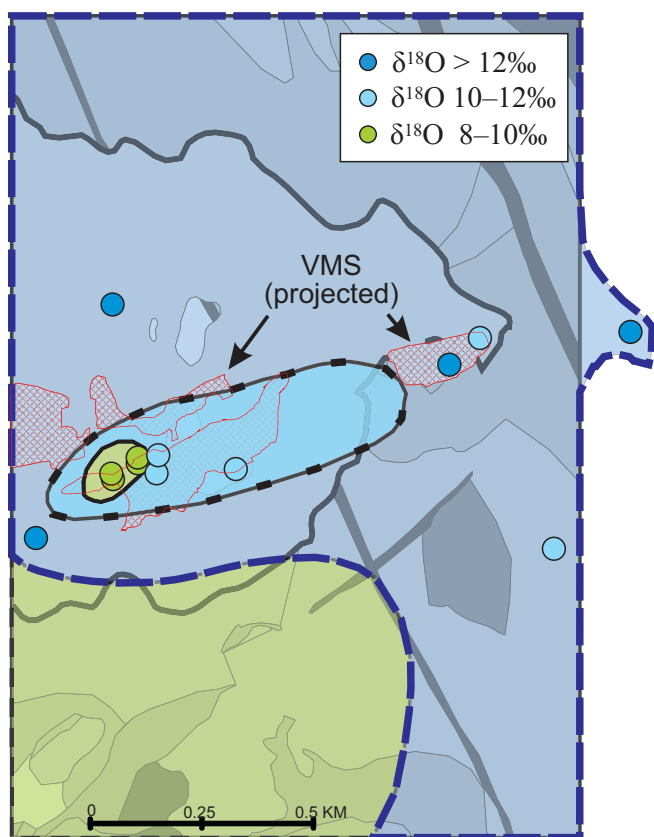relatively lower $\delta^{18}O$. The location of this 'central' zone suggests that it is situated above a footwall upflow zone. The locations of the projected outlines of the larger VMS lenses beneath Izok Lake coincide with the small zone of $\delta^{18}O = 8–10‰$ shown in Figure 9.

Comparison with the Caldera-Hosted Sturgeon Lake VMS District

Oxygen isotope zonation of the Archean Sturgeon Lake caldera and VMS district in northwestern Ontario by Holk et al. (2008) is illustrated in Figure 10. Here, there are high-$\delta^{18}O$ zones in the hanging wall similar to those mapped at Izok Lake. The structural setting of the Sturgeon Lake caldera is such that the very steep, northward dips of the volcanic section provide a cross-section through the caldera.

A shallow, emergent volcanic complex above the Biedelman Bay intrusive complex, led to the development of an extensive, low-temperature, high-$\delta^{18}O$ alteration zone in the hanging wall above the Mattabi VMS deposit. Comparison of the isotopic composition

and placement of the low-temperature oxygen isotope zonation at Sturgeon Lake and Izok Lake is instructive: Sturgeon Lake provides a cross-sectional view, whereas Izok Lake a top-down (plan) view of the high-$\delta^{18}O$, "capping" alteration zone. High-temperature, ^{18}O-depleted upflow zones are present beneath the level of the Mattabi VMS at Sturgeon Lake (Fig. 10). The top-down view of the paleo hydrothermal system at Izok Lake, and the limited deep drilling, limits the access to similar, low-$\delta^{18}O$ upflow zones which must lie deep beneath the Izok deposit. Morrison (2004) reports the occurrence of 'stringer zones' in the footwalls to several sulphide lenses.

An important feature of the Biedelman Bay intrusive complex is that the level of emplacement is very-late to post-hydrothermal. This is indicated by the lack of isotopic alteration of the intrusion at its upper contact, as evidenced by the presence of fresh rock in abrupt contact/juxtaposed with previously-altered, basaltic wallrocks. The Biedleman Bay intrusive complex is genetically related, however, to extrusive rocks deposited higher in the section (Holk et al., 2008).

Oxygen Isotope Zonation and Lithogeochemical Indicators of Alteration

The oxygen isotope zonation patterns, at Izok Lake can be compared with other geochemical, mineralogical, and mineral chemical indicators of hydrothermal alteration. Sodium depletion/removal in bulk rocks is due to the destruction of Na-Ca feldspars in VMS-bearing footwall successions and has long been used as a monitor of hydrothermal alteration (e.g. Franklin, 1997). The distribution of sodium in surface lithogeochemical samples of hanging-wall rhyolite (i.e. R2 rhyolite and younger; R1 rhyolite hosts the VMS lenses: Bailey and Stubley, 2013a,b), mapped as the isopleth of 1% Na_2O, in the Izok Lake area is shown in Figure 11. Rhyolitic rocks within the isopleth contain less than 1% Na_2O (Morrison, 2004). The marked coincidence of this Na depletion zone with the mapped oxygen isotope zones (the >12‰ zone in particular; see also Fig. 9) indicates the large size (several km in diameter) of the zone of rocks that were hydrothermally altered by the Izok VMS-forming hydrothermal system. However, the extensive nature of apparent sodium loss indicated in Figure 11 makes it a less spatially definitive vectoring tool relative to oxygen isotope mapping.

A potentially useful indicator of hydrothermal alteration is the Ishikawa Index (AI = 100(K_2O+MgO)/(K_2O+ MgO+Na_2O+CaO)): Ishikawa et al., 1976), calculated from whole-rock chemical analyses. This index was mapped using lithogeochemical samples collected from outcrops on a regional scale in the Izok Lake area by Laakso et al. (2015) by interpolation of 1241 whole-rock chemical analyses using an inverse distance
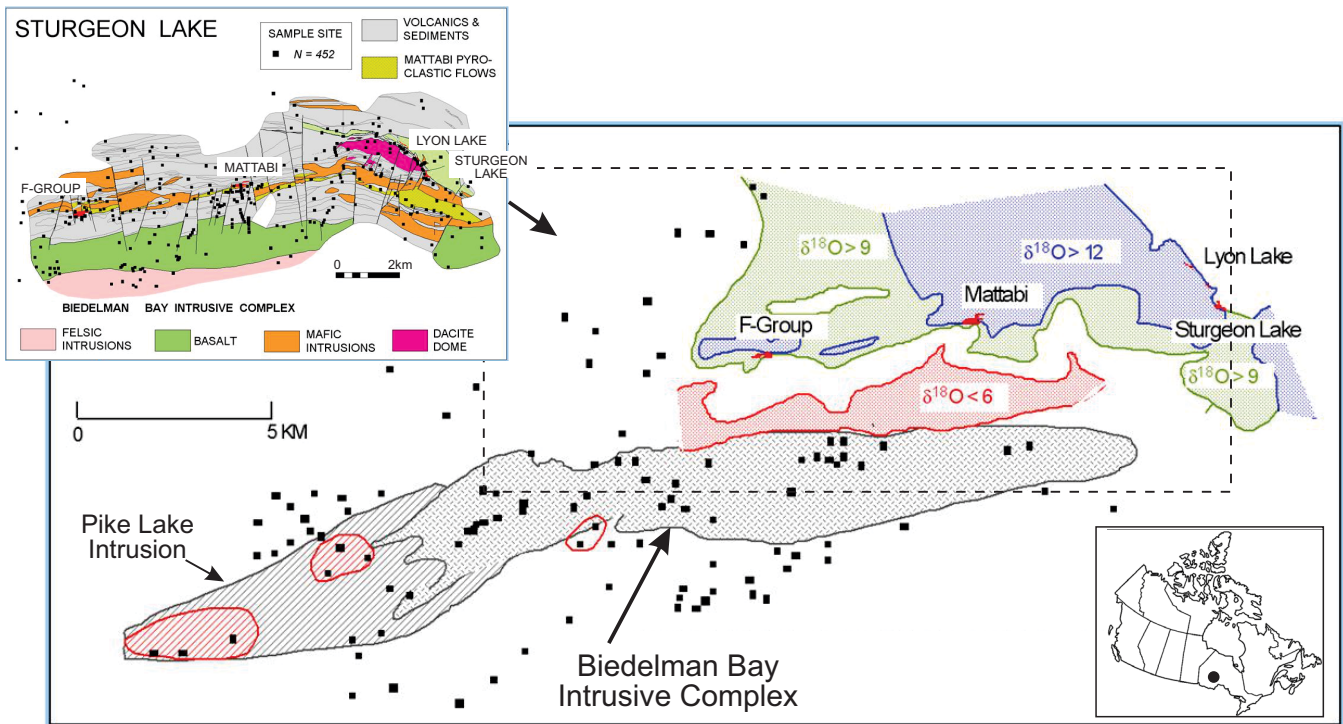
Figure 10. Oxygen isotope zonation above the Biedelman Bay intrusive complex, Sturgeon Lake, Ontario (Holk et al., 2008; geology modified from Franklin et al., 1975), provides an instructive comparison to Izok Lake. The dip of the layered volcanic rocks is nearly vertical; the inset geological map (simplified from Morton et al., 1999) and the map of oxygen isotope zoning are virtual cross-sections depicting both the high-temperature reaction zone and a later, low-temperature alteration of hanging-wall rocks. The geological and hydrothermal history of this caldera complex played an important role in the development of high values of $\delta^{18}O_{WR}$ in the hanging wall (see Holk et al., 2008).

weighting method (IDW; Fig. 11). There is a general correspondence between the region encompassed by the Na_2O depletion isopleth, the oxygen isotope zoning (see also Fig. 8) and the AI. Note, however, that the area suggested from the AI to be the most intensely altered appears to align with the general trend of fold axes and the distribution of VMS lenses. Although the AI map pattern appears to be structurally influenced, and the projected VMS lenses coincide with the intersection of the linear trend of maximum Ishikawa Index (AI) and the central area of high $\delta^{18}O$, the intense alteration (AI) indicated may have been somewhat broader prior to folding. Notably, this zone of high AI correlates spatially with a prominent occurrence of sillimanite-garnet-bearing rocks mapped by Stubley and Bailey (2013, unpub.) likely derived from metamorphism of muscovite-chlorite-bearing alteration assemblages. Whereas, the AI mapped in the Izok Lake area provides an indication of the broad extent of hydrothermal alteration, the more restricted oxygen isotope zonation pattern defines both the upright architecture (geometry) of the paleo-hydrothermal system and an effective 'vector' to mineralization in addition

Oxygen Isotope Zonation and Short-Wave Infrared Reflectance Spectrometry

Ground spectrometric data were acquired in the visible near infrared-short-wave infrared spectral region (VNIR-SWIR) by Laakso et al. (2015) to map the spectral properties of the phyllosilicate minerals in the rhyolitic rocks of the Izok Lake area. These authors focused on the spectral region of the Al-OH absorption feature near 2200 nm associated with white mica, and for the Fe-OH absorption feature (near 2250 nm) associated with biotite and chlorite. Up to eight spectra were measured at each selected outcrop, and averaged to yield a final ground spectral dataset of 285 measurements. A sub-set of these data is used here for comparison with oxygen isotope data for samples collected within 200 m of the same site.

Chlorite and white mica minerals are universally important components of hydrothermally altered of volcanic rocks associated with VMS deposits. Variation in the position of the absorption features for each of these minerals reflects a variation in their chemical composition (Duke, 1994). For example, a shift to longer wavelengths in the position of the Al-OH absorption feature is due to increasing substitution of Mg and Fe for Al (Duke, 1994; Bishop et al., 2008). A similar shift in the Fe-OH position is due to an increase in Fe in chlorite. Laakso et al. (2015) noted a concomitant change in the position on an Alteration Box Plot (Large et al., 2001; a bi-variate plot of AI versus Chlorite-Carbonate-Pyrite Index, or CCPI), with
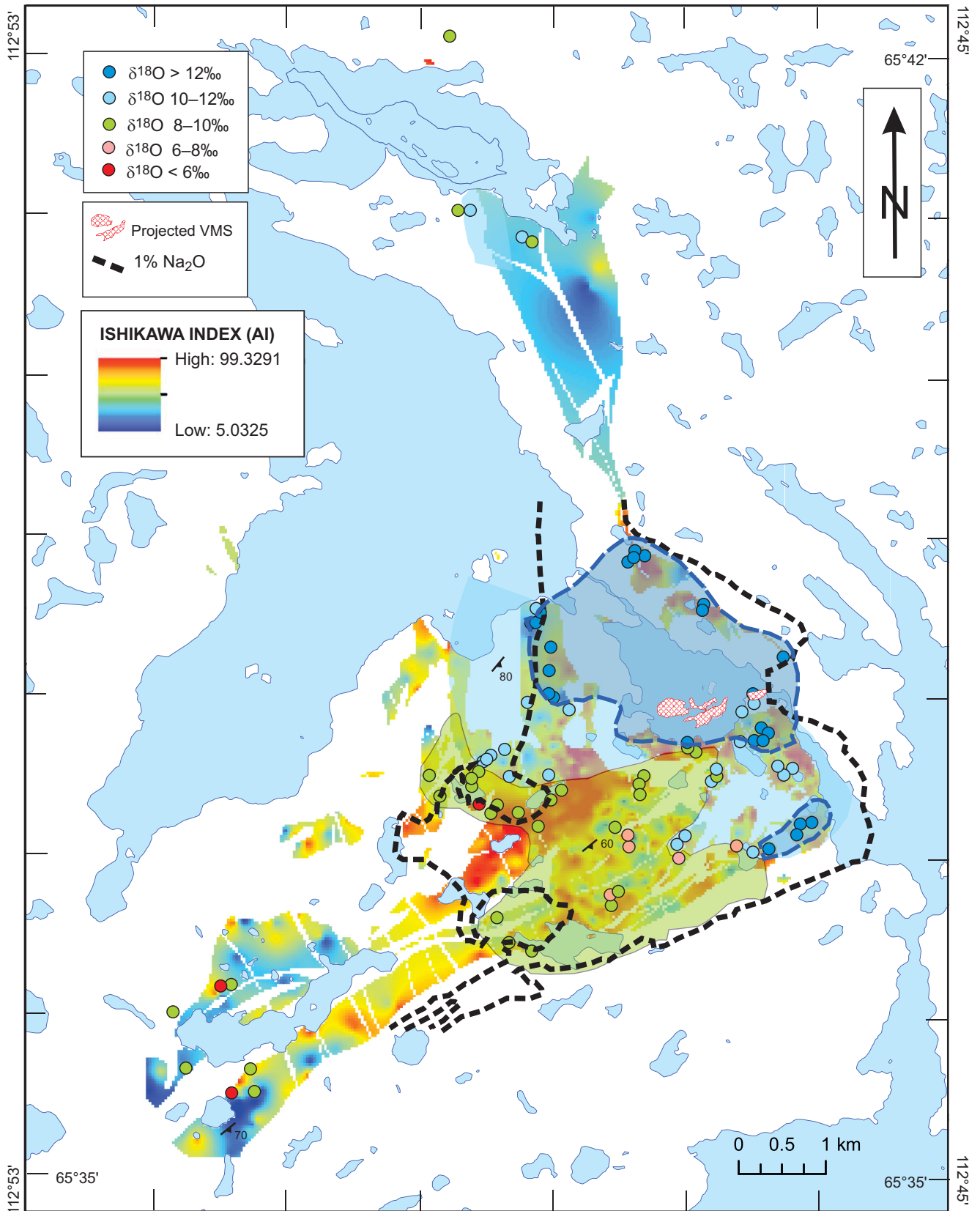
39

Figure 11. Map of the Izok Lake area comparing the oxygen isotope zonation to the location of a <1% Na$_2$O isopleth (Morrison, 2004) and to the variation in rock alteration based on the chemical Ishikawa Index (AI = 100(K$_2$O+MgO)/(K$_2$O+MgO+Na$_2$O +CaO).

increasing wavelength position of the Al-OH absorption feature.

Linear regression of the whole-rock values of $\delta^{18}O$ plotted in Figure 12a indicates a significant correlation with the spectral positions of the absorption features for Al-OH ($R^2 = 0.53$; due to white micas) and Fe-OH ($R^2 = 0.62$; due to chlorite). A shift towards shorter Al-OH absorption feature wavelengths, corresponding to an increase in the Al content of the white micas, was also documented in a biotite- to sillimanite-grade metamorphic progression in rocks from the Belt Supergroup by Duke and Lewis (2010). That is, the Al content increases with increasing temperature of crystallization. Similarly, a slight increase in Al-OH wavelength correlates with an increase in $\delta^{18}O$ (Fig. 12a), which may reflect a decrease in hydrothermal alteration temperature that has been preserved despite subsequent high-grade regional metamorphism. A shift towards longer Al-OH absorption feature wavelengths also appears to coincide with a decrease in alteration intensity (Laakso et al., 2015) in the ground spectral data. In some instances, the Al-OH wavelength/alteration intensity correlation has been inferred to indicate a low-temperature recharge zone (van Ruitenbeek et al., 2005). In the Izok Lake area, however, we do not favour such an interpretation to explain the relatively long Al-OH wavelengths in hanging-wall rocks. Rather, the high-Al-OH wavelengths variations may largely reflect distal, lower temperature waning discharge alteration mineral assemblages that were subsequently recrystallized during regional metamorphism.

The presence of abundant Fe chlorite in the footwall upflow zones (so-called "pipes") of VMS hydrothermal systems (e.g. Larson, 1984; MacLean and Hoy, 1991; Taylor et al., 2014) and high Fe contents of modern high-temperature vent fluids (e.g. Von Damm, 1995) are typically interpreted to be the product of high-temperature, "prograde" hydrothermal circulation and evolution (e.g. van Ruitenbeek et al., 2005). However, in the Izok Lake area, the increase in the wavelength of the Fe-OH absorption feature (indicating an increase in the Fe/(Fe+Mg) ratio of biotite and chlorite) correlates with an increase, rather than decrease, in whole-rock $\delta^{18}O$ (Fig. 12b). This indicates alteration occurred at lower, rather than higher temperatures. Moreover, Laakso et al. (2015) noted an increase in the wavelength of the Fe-OH absorptions of biotite and chlorite near the massive sulphide lenses at Izok Lake. However, in various hydrothermal settings, variations in the Fe/(Fe+Mg) of chlorite are interpreted to be controlled primarily by the composition of the hydrothermal fluid (e.g. Kuroko deposits: Shikazono and Kawahata, 1987; Matagami, Quebec: Kranidiotis and MacLean, 1987; modern geothermal sites: Cathelineau, 1988) and by physical properties of the system (e.g. temperature: Mercier-
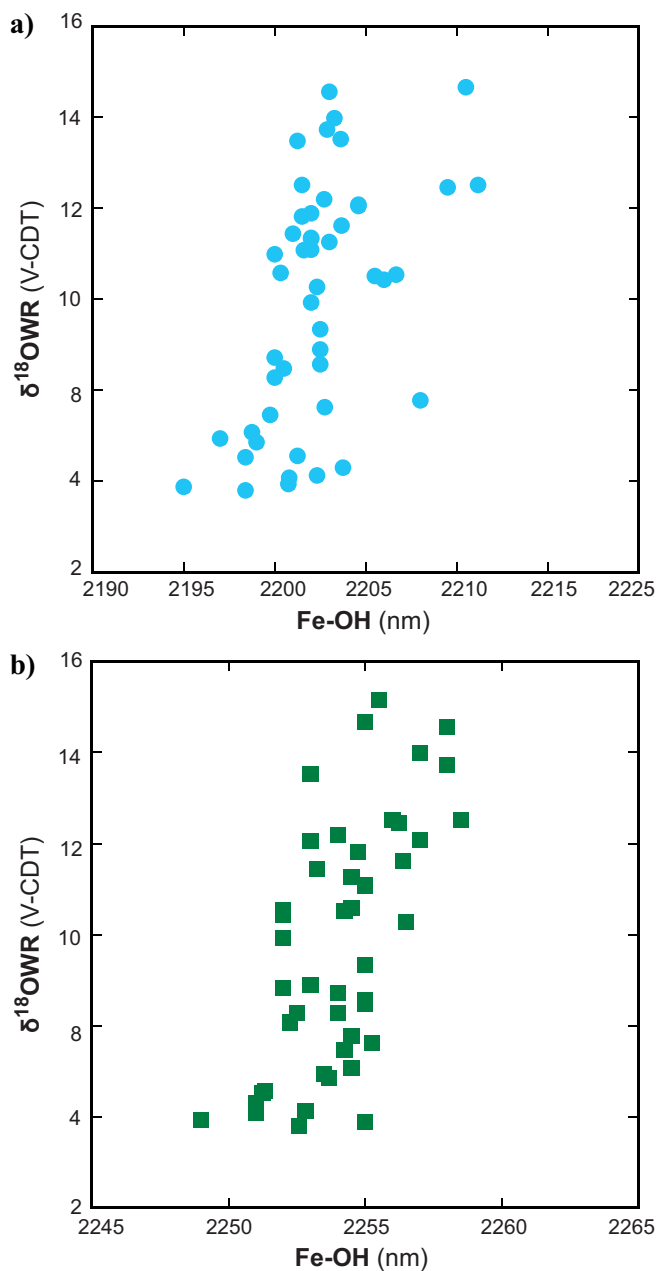
Figure 12. a) Plot of $\delta^{18}O_{WR}$ versus Al-OH absorption feature illustrates a correlation (linear fit, $R^2 = 0.53$) suggesting decreasing mineralogical alteration and increasing paragonite (Na+) substitution in white mica at lower water/rock interaction temperatures. **b)** Plot of $\delta^{18}O_{WR}$ versus Fe-OH absorption feature ($R^2 = 0.62$) implies, unexpectedly, an increase in alteration intensity at lower temperatures (increasing $\delta^{18}O_{WR}$), assuming a marine hydrothermal fluid (i.e. $\delta^{18}O_{H_2O}$ ~0‰).

Langevin et al., 2014). For example, chlorite from low-temperature sericite-chlorite±carbonate assemblages developed near the seafloor (VMS-bearing zone, and immediate hanging wall) at the Lemoine Au-bearing VMS deposit are Fe-rich (Mercier-Langevin et al., 2014). A similar relationship at Izok Lake is consistent with the correlation between $\delta^{18}O$ and the Fe-OH wavelength shown in Figure 12.
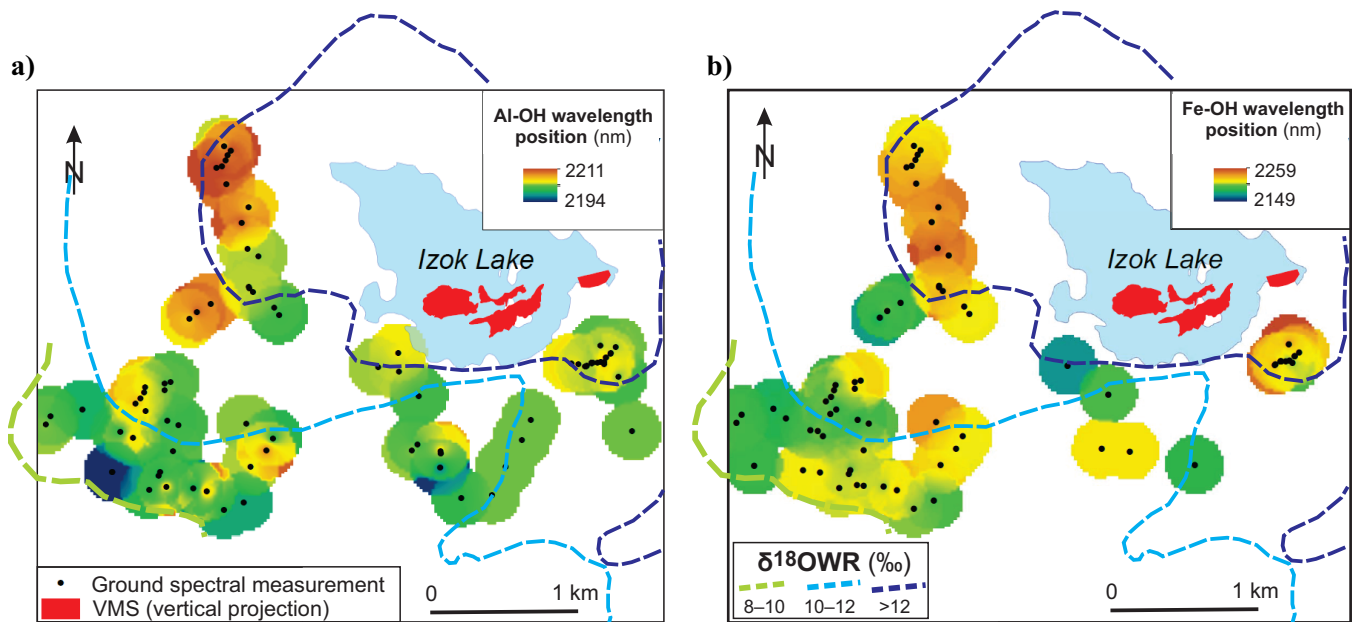
Figure 13. a) Alteration map based on a field-measured, short-wave infrared spectral feature for Al-OH absorption due to white mica. Boundaries of oxygen isotope zones (see Fig. 8) are shown for comparison. **b)** Alteration map based on a field-measured spectral feature for Fe-OH absorption due to chlorite. Increasing wavelength (in nm) is associated with an increase in the Chlorite-Carbonate-Pyrite Alteration Index; CCPI = 100 (FeO+MgO) /(FeO+MgO+Na$_2$O+K$_2$O).

A comparison between the spatial extent of the oxygen isotope zones and measured Al-OH and Fe-OH wavelength positions is shown in Figure 13a,b, respectively. Areas of the longest wavelengths for both Al-OH and Fe-OH absorption features are largely within the zone of highest δ^{18}O. The areas of the longest Al-OH wavelength appear to be concentrated at the outer margins of the high-δ^{18}O zone, although this spatial relationship may result from the location of outcrops selected for measurement. In addition, there is only a slight correspondence between the areas of longest wavelength positions and the area of highest AI (compare Figs. 11 and 13a,b). However, the lack of correspondence may be only apparent, and biased by the distribution and density of measurement sites. A general correspondence between variation in positions of the absorption features and the pattern of oxygen isotope zonation is nevertheless apparent.

IMPLICATIONS FOR EXPLORATION

The paleo-hydrothermal system responsible for the Izok VMS deposit has been effectively mapped using whole-rock oxygen isotope analyses. The distribution of oxygen isotope alteration, mapped in the form of zones, describes a top-down (plan) view of a nearly upright hydrothermal system, with a ^{18}O-enriched 'cap' overlying the VMS deposit that provides a hanging-wall vector to subsurface mineralization. Oxygen isotope zonation based on analytical results for drill core samples collected near and just beneath the VMS deposit indicates the general location of an upflow zone in the footwall.

Because some subvolcanic centres that are prospective for VMS were active through several distinct magmatic episodes, and each could potentially be associated with VMS deposition, explorationists should be aware of the potential presence of multiple, vertically 'stacked' hydrothermal alteration systems and massive sulphide lenses, especially if the subvolcanic centre is large and long-lived. Although a discrete subvolcanic intrusion that would have provided the heat to drive the hydrothermal system in the Izok Lake area has not been identified, our oxygen isotope mapping indicates that the Izok deposit is situated at the top of the related hydrothermal system. On the basis of this study, the presence of a multiple, 'stacked' mineralization-alteration system, with additional sulphide bodies at depth, cannot be ruled out.

Despite subsequent amphibolite-facies metamorphism, the pattern of oxygen isotope alteration zonation remains undisturbed, emphasizing the value of the isotopic technique to exploration, and limited only by the availability and distribution of samples. The oxygen isotope effects of alteration in a seafloor VMS-related system is a robust 'fingerprint' that remains in the rock to the temperature of melting, disturbed only by deformation which will be reflected by the morphology of the oxygen isotope zoning. Therefore, oxygen isotope mapping is a viable tool to determine the location and architecture of a potentially VMS-bearing hydrothermal system. Furthermore, correlation of whole-rock δ^{18}O with spectral data reinforces the utility of a multi-faceted approach to alteration mapping.

ACKNOWLEDGEMENTS

REFERENCES

Ames, D., Galley, A. G., Taylor, B.E., Kjarsgaard, I. M., and Tardif, N., in press. Hanging wall vectoring for buried VMS deposits, Paleoproterozoic Flin Flon mining camp, Manitoba, Canada; Economic Geology.

Bailes, A.H., Galley, A.G., Paradis, S., and Taylor, B.E., in press. Variations in large synvolcanic alteration zones at Snow Lake, Manitoba, Canada, with proximity to associated VMS deposits; Economic Geology.

Bailey, K. and Stubley, M., 2013a. The Izok volcanic-hosted massive sulphide deposit, Nunavut, Canada: A new interpretation of the rhyolitic stratigraphy and implications for exploration, *In:* Abstracts Volume; Society of Economic Geologists Annual Meeting, Whistler, September 24-27, 2013, p. 133 –139.

Bailey, K. and Stubley, M., 2013b. Izok volcanic-hosted massive sulphide deposit, Nunavut, Canada: A new interpretation of the rhyolitic stratigraphy and implications for exploration, *In:* Abstracts Volume Society of Economic Geologists Annual Meeting, Whistler, September 24-27, 2013, p. 44.

Beaudoin, G., Mercier-Langevin, P., Dube, B., and Taylor, B.E., 2014. Low-temperature alteration at the world-class LaRonde Penna Archean Au-rich volcanogenic massive sulfide deposit, Abitibi Subprovince, Quebec, Canada: evidence from whole-rock oxygen isotopes; Economic Geology, v. 109, p. 167–182.

Bishop, J.L., Lane, M.D., Dyar, M.D. and Brown, A.J., 2008. Reflectance and emission spectroscopy study of four groups of phyllosilicates: smectites, kaolinite-serpentines, chlorites and micas; Clay Minerals, v. 43, p. 35–54.

Bleeker, W. and Hall, B., 2007. The Slave Craton: Geological and metallogenic evolution, *In:* Mineral deposits of Canada: A Synthesis of Major Deposit Types, District Metallogeny, the Evolution of Geological Provinces, and Exploration Methods, (ed.) W.D. Goodfellow; Geological Association of Canada, Mineral Deposits Division, Special Publication 5, p. 849–879.

Borthwick, J. and Harmon, R.S., 1982. A note regarding ClF_3 as an alternative to BrF_5 for oxygen isotope analysis; Geochimica et Cosmochimica Acta, v. 46, p. 1665–1668.

Cathelineau, M., 1988. Cation site occupancy in chlorites and illites as a function of temperature; Clay Minerals, v. 23, p. 471–485.

Cathles, L.M., 1993. Oxygen isotope alteration in the Noranda mining district, Abitibi greenstone belt, Quebec; Economic Geology, v. 88, p. 1483–1511.

Davis, W.J. and Hegner, E., 1992. Neodymium isotopic evidence for the tectonic assembly of late Archean crust in the Slave Province, Northwest Canada; Contributions to Mineralogy and Petrology, v. 111, p. 493–504.

Duke, E.F., 1994. Near infrared spectra of muscovite, Tschermak substitution, and metamorphic reaction progress: Implications for remote sensing; Geology, v. 22, p. 621–624.

Duke, E.F. and Lewis, R.S., 2010. Near infrared spectra of white mica in the Belt Supergroup and implications for metamorphism; American Mineralogist, v. 95, p. 908–920.

Franklin, J.M., 1997. Lithogeochemical and mineralogical methods for base metal and gold exploration, *In:* Proceedings of Exploration 97, (ed) A.G. Gubins; Fourth Decennial International Conference on Mineral Exploration, Prospectors and Developers Association of Canada, p. 191–208.

Galley, A.G., Hannington, M.D., and Jonasson, I.R., 2007. Volcanogenic massive sulphide deposits, *In:* Mineral deposits of Canada: A Synthesis of Major Deposit Types, District Metallogeny, the Evolution of Geological Provinces, and Exploration Methods, (ed.) W.D. Goodfellow; Geological Association of Canada, Mineral Deposits Division, Special Publication 5, p. 141–161.

Green, G.R., Ohmoto, H., Date, J., and Takahashi, T., 1983. Whole-rock oxygen isotope distribution in the Fukazawa-Kosaka area, Hokuroku district, Japan; Economic Geology Monograph 5, p. 395−411.

Holk, G.J., Taylor, B.E., and Galley, A.G., 2008. Oxygen isotope mapping of the Archean Sturgeon Lake caldera complex and VMS-related hydrothermal system, Northwestern Ontario, Canada; Mineralium Deposita, v. 43, p. 623–640.

Ishikawa, Y., Sawaguchi, T., Iwaya, S., and Horiuchi, M., 1976. Delineation of prospecting targets for Kuroko deposits based on modes of volcanism of underlying dacite and alteration haloes; Mining Geology, v. 26, p. 105–117.

Kranidiotis, P. and MacLean, W., 1987. Systematics of chlorite alteration at the Phelps Dodge massive sulfide deposit, Matagami, Quebec; Economic Geology, v. 82, p. 1898–1911.

Laakso, K., Rivard, B., and Peter, J.M., 2015. Hyperspectral reflectance spectrometry in the exploration for VMS deposits using the Izok Lake Zn-Cu-Pb-Ag deposit, Nunavut as a test site, *In:* Targeted Geoscience Initiative 4: Contributions to the Understanding of Volcanogenic Massive Sulphide Deposit Genesis and Exploration Methods Development, (ed.) J.M. Peter and P. Mercier-Langevin; Geological Survey of Canada, Open File 7853, p. 15–25.

Large, R.R., Gemmell, J.B., Paulick, H. and Huston, D.L., 2001. The alteration box plot: A simple approach to understanding the relationship between alteration mineralogy and lithogeochemistry associated with volcanic-hosted massive sulfide deposits; Economic Geology, v. 96, p. 957–971.

Larson, P.B., 1984. Geochemistry of the alteration pipe at the Bruce Cu-Zn volcanogenic massive sulfide deposit, Arizona; Economic Geology, v. 79, p. 1880−1896.

MacLean, W. and Hoy, L.D., 1991. Geochemistry of hydrothermally altered rocks at the Horne Mine, Noranda, Quebec; Economic Geology, v. 86, p. 506–528.

Mercier-Langevin, P., Lafrance, B., Bécu, V., Dubé, B., Kjarsgaard, I., and Guha, J., 2014. The Lemoine auriferous volcanogenic massive sulfide deposit, Chibougamau camp, Abitibi, greenstone belt, Quebec, Canada: geology and genesis; Economic Geology, v. 109, p. 231–269.

Morrison, I. R., 2004. Geology of the Izok massive sulfide deposit, Nunavut Territory, Canada; Exploration Mining Geology, v. 13, p. 25–36.

Mortensen, J.K., Thorpe, R.I., Padgham, W.A., King, J.E., and Davis, W.J., 1988. U-Pb zircon ages for felsic volcanism in Slave Province, N.W.T., *In:* Radiogenic Age and Isotopic Studies: Report 2; Geological Survey of Canada, Paper 88-2, p. 85–95.

Piercey, S.J., Chaloux, E.C., Péloquin, A.S., Hamilton, M.A., and Creasar, R.A., 2008. Syn-volcanic and younger plutonic rocks from the Blake River Group: Implications for regional metallo-genesis; Economic Geology, v. 103, p. 1243–1268.

Shanks, W.C. III, 2001. Stable isotopes in seafloor hydrothermal systems - Vent fluids, hydrothermal deposits, hydrothermal alteration, and microbial processes, *In:* Stable Isotope Geochemistry, (ed.) J.W. Valley and D.R. Cole; Reviews in Mineralogy and Geochemistry, v. 43, p. 469–525.

Sheppard, S.M.F. and Taylor, H.P. Jr., 1986. Igneous rocks: III. Isotopic case studies of Magmatism in Africa, Eurasia and Oceanic Islands *In:* Stable Isotopes in High-Temperature Geological Processes, (ed.) J. W. Valley, H.P. Jr Taylor, and J.R. O'Neil; Mineralogical Society of America, Reviews in Mineralogy, v. 16, p. 319–372.

Shikazono, N. and Kawahata, H., 1987. Compositional differences in chlorite from hydrothermally altered rocks and hydrothermal ore deposits; The Canadian Mineralogist, v. 25, p. 465–474.

Stubley, M. and Bailey, K., 2013. Bedrock geology of the southern Izok Lake area, West-central Slave Craton; Unpublished report, MMG Resources, Inc., 52 p.

Taylor, B.E., 2004. Fluorination methods in stable isotope analysis, Chapter 20, *In:* Handbook of Stable Isotope Analytical Techniques, Volume 1, (ed.) P.A. de Groot; Elsevier, Amsterdam, p. 400–472.

Taylor, B.E., de Kemp, E., Grunsky, E., Martin, L., Maxwell, G., Riggs, D., Goutier, J., Lauziere, K., and Dube, B., 2014. Three-dimensional visualization of the Archean Horne and Quemont hydrothermal systems, Blake River Group, Quebec; Economic Geology, v.109, p. 183–203.

Taylor, B. and Holk, G., 1998. Stable isotope applications in the exploration for volcanic-associated massive sulphide deposits: a preliminary summary, *In:* Database for CAMIRO Project 94E07: interrelationships between subvolcanic intrusions, large-scale alteration zones and VMS deposits (ed.) A. Galley, A. Bailes, M. Hannington, G. Holk, J. Katsube, F. Paquette, S. Paradis, F. Santiguida, and B. Taylor; Geological Survey of Canada, Open File 4431, p. 41–46.

Taylor, B.E., Holk, G., Dubé, B., and Galley, A., 2009 Oxygen isotope zoning in subvolcanic, intrusion-centered submarine hydrothermal systems as a guide to VMS exploration, *In:* Proceedings; 24th International Applied Geochemistry Society Meeting, Fredericton, June 1-4, 2009, p. 255–258.

Taylor, B.E. and South, B.C., 1985. Regional stable isotope systematics of hydrothermal alteration and massive sulfide deposition in the West Shasta district, California; Economic Geology, v. 80, p. 2149−2163.

Taylor, B.E. and Timbal, A., 1998a. Regional stable isotope studies in the Snow Lake area, *In:* Database for CAMIRO Project 94E07: interrelationships between subvolcanic intrusions, large-scale alteration zones and VMS deposits (ed.) A. Galley, A. Bailes, M. Hannington, G. Holk, J. Katsube, F. Paquette, S. Paradis, F. Santiguida, and B. Taylor; Geological Survey of Canada, Open File 4431, p. 271–280.

Taylor, B.E. and Timbal, A., 1998b. Regional stable isotope studies in the Noranda Volcanic Complex, *In:* Database for CAMIRO Project 94E07: interrelationships between subvolcanic intrusions, large-scale alteration zones and VMS deposits (ed.) A. Galley, A. Bailes, M. Hannington, G. Holk, J. Katsube, F. Paquette, S. Paradis, F. Santiguida, and B. Taylor; Geological Survey of Canada, Open File 4431, p. 243–252.

Taylor, H.P., Jr., 1968. The oxygen isotope geochemistry of igneous rocks; Contributions to Mineralogy and Petrology, v. 19, p. 1–71.

Taylor, H.P., Jr., 1986. Igneous rocks: II. Isotopic case studies of circumpacific magmatism, Chapter 9, *In:* Stable Isotopes in High-Temperature Geological Processes, (ed.) J.W. Valley, H.P. Taylor Jr., and J.R. O'Neil; Mineralogical Society of America, Reviews in Mineralogy, v. 16, p. 273–318.

Thorpe, R.I., Cumming, G.L., and Mortensen, J.K., 1992. A significant Pb isotope boundary in the Slave Province and its probable relation to ancient basement in the western Slave Province, *In:* Project Summaries, Canada-Northwest Territories Mineral Development Agreement 1987-91, (comps) D.G. Richardson and M. Irving; Geological Survey of Canada, Open File 2484, p. 179–184.

van Ruitenbeek, F.J.A., Cudahy, T., Hale, M., and van der Meer, F. D., 2005. Tracing fluid pathways in fossil hydrothermal systems with near-infrared spectroscopy; Geology, v. 33, p. 597–600.

Von Damm, K.L., 1995. Temporal and compositional diversity in seafloor hydrothermal fluids; Reviews in Geophysics, v. 33, Supplement Part 2, p. 1297–1305.